journal

J. Am. Ceram. Soc., 98 [9] 2681–2688 (2015)
DOI: 10.1111/jace.13753

Toward Demystifying the Mohs Hardness Scale

William W. Gerberich,[‡,†] Roberto Ballarini,[§,†] Eric D. Hintsala,[‡] Maneesh Mishra,[¶] Jean-Francois Molinari,[‖] and Izabela Szlufarska[††]

[‡]University of Minnesota, Department of Chemical Engineering and Materials Science, Minneapolis, Minnesota

[§]University of Houston, Department of Civil and Environmental Engineering, Houston, Texas

[¶]Micron Technology Inc, Boise, Idaho

[‖]Institute of Civil Engineering, Ecole Polytechnique Federale de Lausanne, Lausanne 1025, Switzerland

[††]University of Wisconsin – Madison, Department of Materials Science and Engineering, Madison, Wisconsin

Today, the Mohs scale is used profusely throughout educational systems without any persuasive understanding of the fundamental principles. Why one mineral has a scratch hardness over the next culminating in a scale of 1 (chalk) to 10 (diamond) has no atomistic or structure-sensitive basis that explains this outcome. With modern computationally based atomistic and multiscale models, there is increasing promise of defining the pressure and rate-dependent parameters that will allow a fundamental understanding of the Mohs scale. This study principally addresses the combined fracture and plasticity parameters that qualitatively affect fracture at the nanoscale. A physical model wherein the crack tip under a scratch is shielded by dislocations is supported by molecular dynamics (MD) simulations in both ductile aluminum and brittle silicon carbide. Next, this model is applied to nanoindentation data from the literature to produce a ranking of Mohs minerals based on their fundamental properties. As such, what is presented here is a first step to address the flow and fracture parameters ultimately required to provide a figure of merit for scratch hardness and thus the Mohs scale.

I. Introduction

The Mohs scale was introduced almost 200 yrs ago as a simple way to rank mineral hardness.[1] Since then, multiple scientific papers from mathematical physicists,[2] physical chemists,[3] civil engineers,[4] and materials scientists[5] have debated the role of plasticity and fracture on scratch hardness and ultimately the Mohs ranking. After the adoption of the Mohs scale, there was little progress in understanding the necessary materials science represented by the seminal contributions to fracture mechanics of Griffith[6] and to dislocation plasticity of Taylor[7] that are prescient to the hypotheses presented here. It is proposed that the next breakthrough point was the bold contribution of David Tabor[3] who proposed that scratch hardness was controlled by properties associated with plastic deformation. Up until then, most agreed that all of the MOHS minerals were brittle with little if any plastic deformation. Tabor's paper was followed by others, including a significant work in 1982 by Trepied and Doukhan at the Universite' Lille who discussed that scratches nucleated plastic deformation via dislocations *in all MOHS minerals*.[8] Significant progress toward the understanding of a type of scratch test used by the geotechnical engineering community in drilling applications was made by Richard et al.,[9] who demonstrated that the compressive strength of rock can be inferred by making scratches shallow enough to prevent significant chipping. These authors recognized that the compressive strength would not be measured for deep scratches, which could be associated instead with fracture toughness. The transition from ductile to brittle fracture in similar applications was shown through simulations by Huang and Detournay[10] to be modulated by the rock material length scale involving the nominal compressive strength and fracture toughness. More recently, Akono, Reis and Ulm at MIT[11] published a paper in Phys. Rev. Lett. stating that scratching is *fracture dominated* using a simple continuum fracture mechanics model. Within 2 yrs, a rebuttal was published[12] showing several reasons why the generality of being able to predict fracture toughness using a scratch test might be limited to special cases of deep cuts and scratches that produced cracks parallel to a cutter prolongation. This, which is more in line with the work of Huang and Detournay, is relevant to this study as many researchers[5,13–16] report predominant cracks from scratches on Mohs minerals to be perpendicular to the scratch groove rather than being parallel to it. The history of the Mohs scale demonstrates that the properties

D. J. Green—contributing editor

Manuscript No. 36544. Received March 10, 2015; approved June 12, 2015.
[†]Authors to whom correspondence should be addressed. e-mails: wgerb@umn.edu and rballarini@uh.edu

Feature

governing scratch hardness are still mysterious. The simple model to be presented here is not proposed to be the definitive answer but will be demonstrated to represent an important step toward understanding the Mohs scale.

II. Background

This model addresses the initiation of damage in a crystal or the first grain of a polycrystalline array where both deformation and fracture causes cracking. At increasingly larger scales, this could easily lead to branched cracking causing more macroscopic separation of material at deeper scratches. Our hypothesis is that both plasticity and fracture are an integral part of any model that proposes to "demystify" the Mohs scale. Many empirical attempts have been proposed leading to a characterization of resistance, R, to scratching or wear, W, as

$$R \simeq W^{-1} \sim K_{IC}^{m} H^{n} \tag{1}$$

where m and n are 1;1,[17] ¾;½,[18] 4/3;−1/9[19] depending on the types of measurements and material classes evaluated. Here, K_{IC} is the plane strain fracture toughness and H is the hardness, often related to the yield or flow strength by a proportionality constant of approximately 2–3. A number of other theoretical attempts have been made involving elastic strain energy density,[20] linear elastic fracture mechanics,[21] and a proposed correlation to surface energy.[22] Most recently, a long-needed study of the Mohs minerals was conducted by Broz, Cook, and Whitney,[5] wherein K_{IC}, H, and indentation elastic modulus, E^*, were measured by nanoindentation and microindentation (Vickers). They concluded there was no simple progression of any one or combination of parameters that could simply explain the Mohs scale. The recently proposed concept[23] that hardness should be strongly related to $(\gamma_s \mu)^{1/2}$, where γ_s and μ are the Griffith surface energy and shear modulus, is consistent with Eq. (1) as this parameter is proportional to fracture toughness. With relatively recent collections of material parameters,[5,8,21,23–62] this has some credibility in Fig. 1. While the correlation is strongly implied, virtually all values of observed K_{IC} are greater than those calculated from surface energy considerations alone. Except for the lowest fracture toughness material, there appears to be a nearly uniform factor of two increases in the apparent K_{IC} over the value associated with the Griffith surface energy concept indicating an additional energy dissipation process. Nevertheless, the fact that cracking occurs in the state of stress associated with scratching even in tougher intermetallics,[63] indicates that the fracture process is also integral to the Mohs hardness scale. Such a depiction along with scratch-induced fractures of Al_3Sc is shown in Figs. 2(a) and (b).

The apparent toughness can be reconciled with the Griffith energy by admitting the presence of dislocation shielded cracking, which is an appropriate physical mechanism for combining brittle fracture and plastic energy dissipation into the scratching or indentation process. This led us to proposing a simple model for hardness based on plasticity, elasticity, and fracture. Recently, this has been applied to known literature for the fracture toughness of oxides, nitrides, carbides, silicates, and diamond.[5,8,21,25–62] Such a model is schematically shown in Figs. 2(c) and (d). As shown in Fig. 2(c), a conical indenter with a spherical tip comes in contact with a surface, exceeding the theoretical stress for dislocation nucleation, τ^{y}_{theo}, where y denotes yield. Several dislocation loops are nucleated on an inclined slip plane with the leading edge component outpacing the trailing screw components. In the second view, Fig. 2(d), a second slip plane is activated by the stress concentration at the contact edge. These two parallel slip planes, as observed in transmission electron microscopy,[24] can be only a few nanometers apart. At the same time a crack is nucleated, with the crack-front driving force

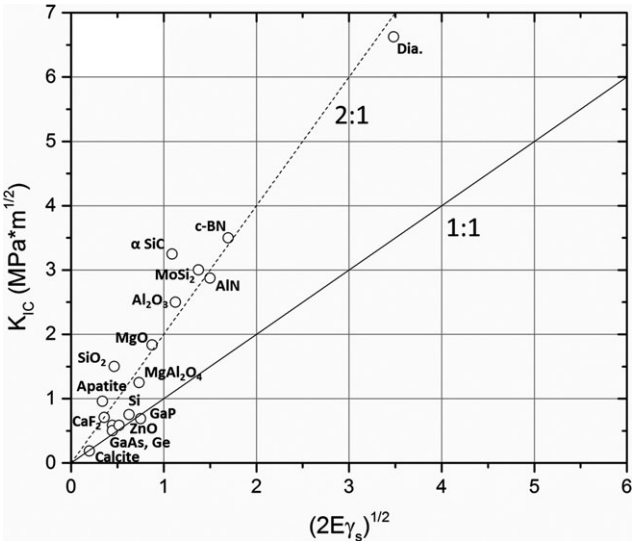

Fig. 1. Comparison of $[2E\gamma_s]^{1/2}$ to K_{IC}.

in equilibrium with the resistive forces of the lattice and the shielding forces of the emitted dislocations. With further loading crack-tip forces can exceed discretized dislocation forces causing instability at τ^{f}_{theo}, where f denotes fracture. It is this incipient fracture toughness, K_{IC}, that we propose can be modeled by the combined properties of elasticity, plasticity, and flow stress (or hardness).

The essential question being explored in this study can be posed by considering the relationship of materials properties to fracture toughness. At the high end of the hardness scale we have low fracture toughness due to low ductility and at the low end we have low fracture toughness due to low modulus and viscosity. In between, there are instances of very high modulus and the highest ductility, which maximize fracture toughness. Based on these observations, the natural question is how to assess where in this general classification scheme the hardness scale switches over from a dependency on the plastic resistance to a dependency on the elasticity and fracture resistance. The opposing hypothesis offered here is that all three properties are ever present in this classification scheme, which does not require some spline fit as a new mechanism kicks in.

Several recent events have led to the hypothesis that either a gradual or nearly discontinuous change in properties can be accommodated by a concept that includes plasticity, elasticity, and fracture toughness. This is not a new concept as many have attempted, both experimentally[55,64,65] and theoretically,[20,21] to explain more fundamentally the concept of hardness. It appears, however, that there have been no successful attempts to explain hardness in terms of elastic, plastic, and fracture (or surface energy) parameters. The well-defined role of plasticity in Mohs hardness, besides the original study of Tabor,[3] has been debated even in the last few years.[11,12] Recently, both experimentally[55,66–68] and theoretically,[69] it has been shown that dislocation plasticity accompanies or precedes fracture of ceramic and mineralogic materials. Room-temperature dislocation microplasticity has been shown from indentations into Al_2O_3,[70] $MoSi_2$,[55] 6HSiC,[65] and MgO.[68] Most recently, Sumiya, et al.[66] have shown room-temperature dislocation plasticity in barium/cadmium mixed oxalate crystals and high-quality synthetic diamond. Probably most telling was the careful experimental study by Page et al.[65] which demonstrated by back-thinning of films previously nanoindented that dislocation emission preceded microcrack formation in 6HSiC. In large-scale computation of 3CSiC, this sequence was later simulated atomistically by Kikuchi et al.[69] who showed that dislocation nucleation preceded fracture. In our own study of silicon nanospheres,[71]

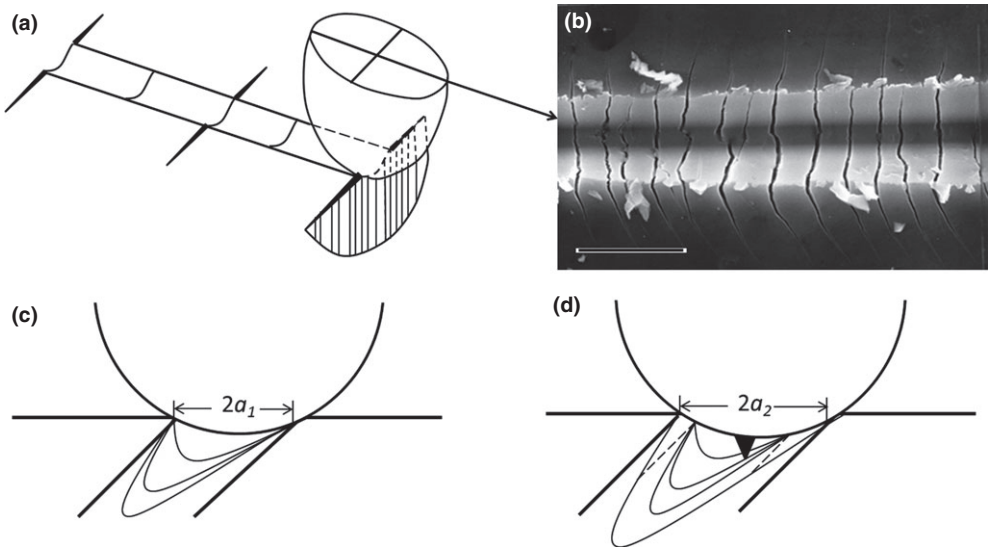

Fig. 2. The role of plasticity and fracture together during scratching: Normal loads would not induce cracking in Al_3Sc but as depicted in (a) a lateral scratch would as shown in (b) (scale bar 10 μm); An indenter contacts a surface to nucleate dislocations in (c) at τ^{y}_{theo} on an inclined slip plane. A parallel source nucleates in (d) at higher loads. This increased load is sufficient to exceed the theoretical stress for fracture, τ^{f}_{theo}.

and more recently, nanocubes,[72] a clear demonstration of residual plastic deformation with no evidence of fracture at over 50% strain in an *in situ* transmission electron microscope compression experiment was found. These observations in silicon nanospheres led to a model correlating the crack extension force or fracture toughness for semiconductors and ceramics to modulus and yield strength. This is given by[23]

$$K_{IC} = \frac{4}{3}\sqrt{\frac{\mu\sigma_{ys}Nb}{1-\nu}} \tag{2}$$

with σ_{ys} the yield stress, b the Burgers vector, and N the number of geometrically necessary dislocations that accommodate the nonrecoverable indenter displacement. Here, we propose that the model presented in Eq. (2) has much broader implications and can be applied to a variety of Mohs minerals. First, results from molecular dynamics simulations will be used to verify the physical model presented in Fig. 2 and thereby the application of Eq. (2) to a more diverse set of materials. Then we will present a ranking of Mohs minerals based on nanoindentation-derived properties for verification.

III. Results and Discussion

(1) Molecular Dynamics Simulations

The relationship between nanoscratching and plasticity has been recently addressed through molecular dynamics in aluminum.[4] Together with Tabor's original hypothesis,[5] the concept of Eq. (1) has some qualitative credibility for Mohs hardness as wear and scratch hardness are conceptually related. Here, we demonstrate a dislocation pile-up of loops at the leading edge of a scratch in an aluminum simulation box. The scratching simulations included in this study combine molecular dynamics (MD) simulations with molecular statics (MS) minimizations and have the same basic setup, shown in Fig. 3. The system is composed of a rigid spherical indenter and a deformable block-shaped substrate which are modeled by aluminum atoms governed by the embedded atom model Mishin potential.[73]

For the simulated scratch test in aluminum, the indenter is dragged at constant speed of 10 nm/ns in the [100] direction and indentation depth of 2 nm for a distance of 10 nm at room temperature. A 2 nm layer of atoms at the bottom of the simulation box is kept fixed as a rigid boundary (blue region in Fig. 3). Another layer of atoms (red region in Fig. 3) maintains the temperature using the Langevin thermostat. For more information see Ref. [74].

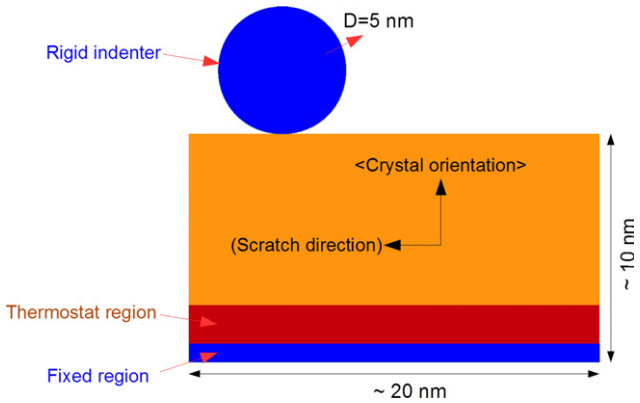

Fig. 3. Schematic simulation setup and related parameters.

The dislocation network underneath the scratching path is visualized by centro-symmetric parameter in OVITO software.[75] In Fig. 4(a), the dislocation network is shown where atoms are colored based on their centro-symmetric parameter, whereas atoms with perfect FCC lattice have been removed. In addition, dislocations have been depicted in Fig. 4(b) using the Dislocation Extraction Algorithm.[76]

The concept of dislocation-shielded cracking under scratch conditions was explored in a much more brittle material. Molecular dynamics simulations of silicon carbide were carried out using in-house codes with Vashishta's empirical potential.[77] This potential has been shown to correctly reproduce melting temperature, dislocation structures, stacking fault energy and cohesive energies of zinc-blende, and hexagonal phases of SiC, as well as high-pressure phase transformation to the rocksalt structure. Elastic constants predicted by our simulations are C_{11} = 390.1 GPa, C_{12} = 142.1 GPa, C_{44} = 133.6 GPa.

For the SiC simulations the sample size is 390 Å × 350 Å × 400 Å. The tip, with a spherical geometry with a 10 nm radius of curvature, is made of amorphous SiC. During sliding simulations, the atoms of the tip are not allowed to relax (the tip is rigid) and only repulsive interactions between the tip and the samples are included. The addition of adhesive forces is not expected

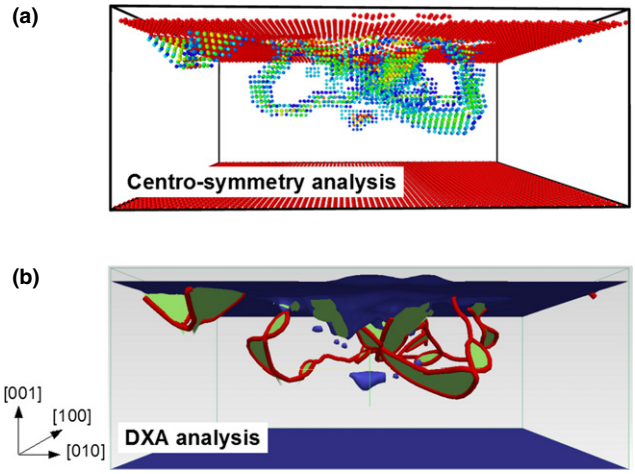

Fig. 4. Dislocation network in single crystalline Aluminum under scratch test: a) atomistic view: Atoms are colored based on the centro-symmetric parameter and FCC atoms are removed. b) Dislocation lines (red), stacking faults (blue), and surfaces (gray) are shown using dislocation extraction algorithm (DXA). The scratch test has been performed in [100] direction on (001) plane.

to change the deformation mechanisms, although it will change the measured normal and lateral forces. The tip is sliding over the (110) surface along the $[1\bar{1}0]$ directions. Atoms in the bottom 2 nm region and 2-nm-thick vertical region far away from the sliding tip are kept fixed to provide rigid boundaries. Sliding velocity is 50 m/s. Temperature of the system is maintained close to 300 K using the Langevin thermostat.

Dislocations are visualized using the shortest-path ring analysis.[78] In simulations, dislocations were found to glide on the $\{111\}\frac{1}{2}\langle 110\rangle$ slip systems. Details of the dislocation dynamics can be found in Ref. [79] The average normal and lateral (friction) forces for the sliding conditions shown in Fig. 5(b) are 2.1 and 0.24 μN, respectively.

Next we explore the plasticity/fracture interactions to facilitate understanding the complexity of a lateral scratch. For the case of low hardness and low modulus materials it is clear that plasticity or viscoelasticity would precede any fracture, but it is not so clear for high hardness and modulus materials. With these atomistic simulations, we illustrate that dislocation nucleation precedes any fracture, as one might expect for aluminum in Fig. 5(a). However, even in Si[72] and SiC,[79] which are quite brittle, plasticity precedes fracture. With an amorphous SiC indenter scratching a 3C zinc blende structure of silicon carbide, similar dislocation loops being emitted are seen in Fig. 5(b). This and other experimental evidence lead to the proposed hypothesis that both dislocation emission and fracture are necessarily involved in scratch testing crystalline materials. It is worth noting that these simulations do not fully capture the effects of length scale, strain rate and image forces and as such it is premature to quantitatively be incorporated in the analysis presented here. However, these results strongly support the physical interpretation of scratch hardness being dictated by both fracture and plasticity through dislocation-shielded cracks underneath the scratch.

(2) Ranking Mohs Minerals by Their Properties

Having provided evidence of the importance of both plasticity and fracture to scratch hardness, an appropriate way to rank Mohs minerals based on properties governing these processes is presented. For 15 relatively brittle substances including diamond, applying Eq. (2) predicted indentation measured values of K_{IC} with a single value of $N = 12$. To obtain a more precise accounting of how relevant such a relationship might be, previously published data for flow and fracture of silicon nanospheres were used. Measured values of compressive yield stress, fracture toughness and both a zero pressure and a pressure corrected form of the shear modulus were utilized in Table I. Pressure corrected moduli following the Murnaghan relationship, as utilized elsewhere,[79, 80] may overcompensate as these nanospheres are not under pure hydrostatic compression. Nevertheless, the result in Fig. 6(a) for six silicon nanospheres,[71,80,81] bulk silicon[81] and two forms of diamond,[5,23,82] natural and nearly

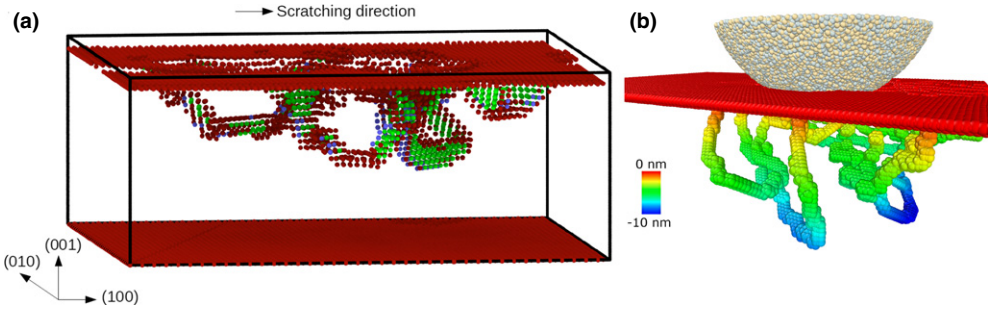

Fig. 5. Atomistic simulations showing plasticity during scratching: (a) Dislocation network in single crystalline Aluminum submitted to a scratch test. (b) Molecular dynamics simulations of sliding friction. SiC sample scratched on (110) surface along the $[1\bar{1}0]$ direction at the average load of 2.1 μN. Dislocations are visualized using shortest-path ring analysis and color corresponds to the depth under the surface.

Table I. Correlations for Silicon Single Crystal Bulk and Nanospheres Without and with Pressure Corrected Moduli

Silicon type	E (Gpa)	μ (Gpa)	ν	b (nm)	H (Gpa)	σ_{ys} (Gpa)	τ_{ys} (Gpa)	K_{IC} (MPa·m)$^{1/2}$	$[\mu\sigma_{ys}b]^{1/2\dagger}$ (MPa·m)$^{1/2}$	$[\mu\sigma_{ys}b]^{1/2\dagger}$ (MPa·m)$^{1/2}$
Bulk	160	60.5	0.218	0.236	12.0	4.0	2.67	0.70	0.247	—
216 nm dia.	197	80.9		0.236	—	5.6	3.74	0.80	0.283	0.327
93 nm dia.	207	85.0		0.236	—	9.2	6.14	1.09	0.362	0.429
63.5 nm dia.	248	102		0.236	—	16.2	10.8	1.98	0.480	0.623
50.2 nm dia.	323	133		0.236	—	31.2	20.8	3.10	0.666	0.986
44 nm dia.	317	130		0.236	—	32.5	21.7	3.07	0.680	0.997
38.6 nm dia.	363	149		0.236	—	45.7	30.5	3.97	0.806	1.26

†The second to last column uses 60.5 GPa for the shear modulus, whereas the last column uses the pressure corrected value, μ_m, from the Murnaghan relation.

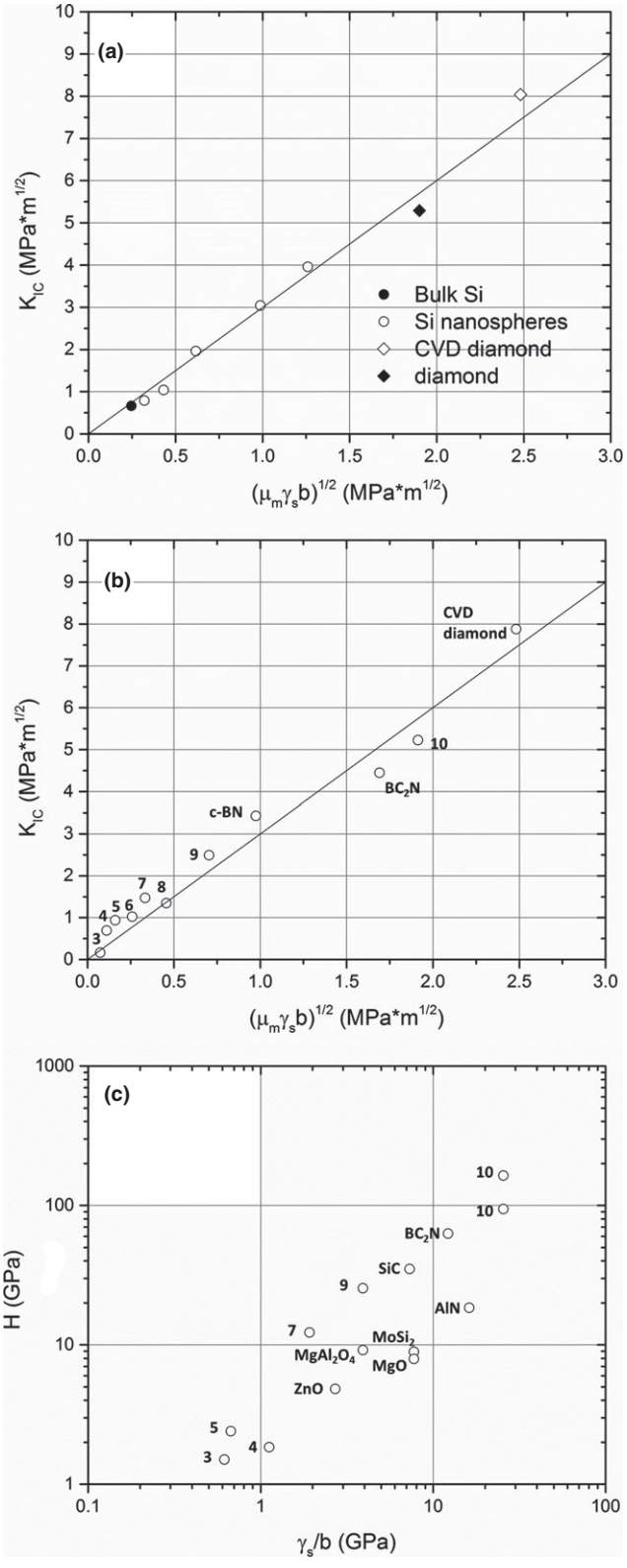

Fig. 6. Correlation of materials properties that define the Mohs ranking: (a) Correlation of K_{IC} to modulus, yield stress, and the Burgers vector based on Eq. (2); A Mohs scale (b) for fracture toughness of 8 Mohs minerals and two superhard cubic boron carbonitrides; (c) correlation for hardness of 6 Mohs minerals and seven additional carbides, nitrides, oxides, and silicides.

defect-free chemical vapor deposited, is remarkable. The number of shielding dislocations that would be needed to satisfy Eq. (2) is 9. It is not a coincidence that the permanent displacement in these nanospheres at the time of fracture was 4.6 ± 1 nm on average representing 19 dislocations if Nb were taken as the normal displacement, which considering there are two contact surfaces matches well.

As both diamond and corundum were both included in the original study[23] and these are both Mohs minerals, this led us to the ultimate conclusion that all of the Mohs minerals might conform to such a criterion. Fracture toughness values for Mohs minerals were only reported for those with hardness values ranging from 3 to 10 due to either no radial cracks forming for talc (Mohs = 1) or inconsistency in gypsum (Mohs = 2).[3] Two extremely hard materials, cubic BC_2N and CVD grown diamond are included at the high hardness end. With the collected data,[5,8,21,23–62] the Mohs fracture toughness prediction gives Fig. 6(b), which is not quite as linear as Fig. 6(a). It also requires $N = 6$ to be consistent with Eq. (2) which is easily within the validity of this approximation.

Returning to the original question of what hardness is, the case is made that for very hard minerals, oxides, nitrides, carbides, and semiconductors, it is the combined resistance to penetration composed of deformation and fracture. This is particularly relevant to scratching where the strain energy release rate is absorbed by a combination of plowing and cracking. As hardness is proportional to flow stress, the simplest of interpretations from Eq. (2) is that

$$H = \alpha' K_{IC}^2/\mu Nb \tag{3}$$

Given that atomistic simulations would rather deal with surface energies,[15] as $K_{IC}^2 \sim 2E\gamma_s$ for a Griffith relation, which can be modified to account for plasticity by replacing γ_s with γ_{eff} (described later) and $E = 2(1 + \nu)\,\mu$ for isotropic elasticity, with $\alpha' = 5.5/\tan\theta$ as a lower bound,

$$H = 36\gamma_{eff}/Nb\tan\theta \tag{4}$$

Here, Nb is the surface displacement required to nucleate cracking and θ is the angle between the emitted dislocation array and the normal to the surface. Figure 6(c) shows the correlation to have a scatter band of a factor of six for hardness. Values of N tan θ would need to vary between 5.5 and 30 to validate Eq. (4) for nanoscratching. This is not unrealistic considering the variations in slip systems activated, in crystal orientations probed, and in the Peierls–Nabarro forces required. Thus, the combination of Eqs. (2) and (4) are proposed to represent the materials properties relationships needed to reproduce the ranking present in the Mohs scale. To fully explain a size effect that is implicit in Eq. (4), one can examine the original paper[23] which can be used to show that the total plastic Tabor[3] strain to nucleate fracture was double for the smaller nanoparticle of 39 nm versus the larger 216 nm one. Specifically, the plastic strains were 0.29 versus 0.145. At such strain levels, γ_s would be replaced by γ_{eff} which would include both surface energy and plastic energy dissipation. As a result, this alone would give a size effect as γ_{eff} would be greater for the smaller particle. Here, γ_{eff} is the strain energy density times the unit volume per sphere area fracture. In addition, the number of dislocations contributing to hardening in the smaller particle would be less, such that the ratio of γ_{eff}/N in Eq. (4) would be larger. Note this is a qualitative argument and detailed discretized dislocation simulations would be required to confirm this. Because of the large local pressures that can be developed in nanoindentation or nanoparticle compression, the Murnaghan[83] relation for pressure corrected modulus was also used in Table I. This strongly suggests that hardness is a combination of a fundamental parameter, γ_s, a material length scale, b, an orientation factor, and the number of dislocations emitted along with their shielding effectiveness. Considerably more research is needed to identify how effective such shielding is in different material classes. In addition, more sophisticated models using unstable stacking energies[84] and a more

self-consistent model appropriate to both ductile and brittle behavior should be examined.

IV. Summary

To summarize, it has been demonstrated that a Mohs fracture toughness scale ranks the Mohs minerals and is strongly connected to the fundamental elastic-plastic and fracture properties of the minerals. This in turn leads to a proposed relationship for hardness of such brittle materials as connected to the surface energy and plastic surface displacement to nucleate cracking in a scratch mode. Together, these are proposed as a basis for the Mohs hardness scale.

Acknowledgments

This research was funded through NSF grant number CMS-0322436, and CMMI -1361868. The authors thank Aghababaei Ramin for his aid with aluminum scratch simulations and input for general discussions

References

[1]F. Mohs, *Treatise on Mineralogy* (Trans. W. Hardinger), pp. 300–7. Caledonian Mercury Press, Edinburgh, 1925.
[2]B. Bhushan, J. N. Israelachvili, and U. Landman, "Nanotribology: Friction, Wear and Lubrication at the Atomic Scale," *Nature*, **374**, 607–16 (1995).
[3]D. Tabor, "The Hardness of Solids," *Rev. Phys. Technol.*, **1**, 145–79 (1970).
[4]T. Junge and J. F. Molinari, "Molecular Dynamics Nano-Scratching of Aluminum: A Novel Quantitative Energy-Based Analysis Method," *Procedia IUTAM*, **3**, 192–204 (2012).
[5]M. E. Broz, R. F. Cook, and D. L. Whitney, "Microhardness, Toughness, and Modulus of Mohs Scale Minerals," *Am. Miner.*, **91**, 135–42 (2006).
[6]A. A. Griffith, "The Phenomena of Rupture and Flow in Solids," *Philos. T. R. Soc. Lond*, **221**, 163–98 (1921).
[7]G. I. Taylor, "Mechanism of Plastic Deformation of Crystals," *P. R. Soc. Lond. A-Conta*, **145**, 362–87 (1934).
[8]L. Trepied and J. C. Doukhan, "Transmission Electron Microscopy Study of Quartz Single Crystals Deformed at Room Temperature and Atmospheric Pressure by Indentations," *J. Phys. Lett.-Paris*, **43**, 77–81 (1982).
[9]T. Richard, F. Dagrain, E. Poyol, and E. Detournay, "Rock Strength Determination from Scratch Tests," *Eng. Geol.*, **147–148**, 91–100 (2012).
[10]H. Huang and E. Detournay, "Intrinsic Length Scales in Tool-Rock Interaction," *Int. J. Geomech.*, **8**, 39–44 (2008).
[11]A. T. Akono, P. M. Reis, and F. J. Ulm, "Scratching as a Fracture Process: From Butter to Steel," *Phys. Rev. Lett.*, **106**, 204302, 4pp (2011).
[12]J. S. Lin and Y. Zhou, "Can Scratch Tests Give Fracture Toughness?" *Eng. Fract. Mech.*, **109**, 161–8 (2013).
[13]M. V. Swain, "Microfracture About Scratches in Brittle Solids," *P. Roy. Soc. Lond. A Mat.*, **366**, 575–97 (1979).
[14]B. R. Lawn, A. G. Evans, and D. B. Marshall, "Elastic/Plastic Damage in Ceramics: The Median/Radial Crack System," *J. Am. Ceram. Soc.*, **63**, 574–81 (1980).
[15]J. D. B. Veldkamp, N. Hattu, and V. A. C. Snijders, "Crack Formation During Scratching of Brittle Materials," *Fract. Mech.*, **3**, 273–301 (1978).
[16]K. Li, Y. Shapiro, and J. C. M. Li, "Scratch Tests of Soda-Lime Glass," *Acta Mater.*, **46**, 5569–78 (1998).
[17]S. M. Hsu and M. Shen, "Wear Prediction of Ceramics," *Wear*, **256**, 867–78 (2004).
[18]A. G. Evans and T. R. Wilshaw, "Quasi-Static and Solid Particle Damage in Brittle Solids – I. Observations, Analysis and Implications," *Acta Metall.*, **24**, 939–56 (1976).
[19]R. W. Ruff and S. M. Weiderhorn, *Erosion by Solid Particle Impact in Treatise on Materials Science and Technology*, Vol. 16, pp. 69–126, Edited by C. M. Preece. Academic Press, New York City, New York, 1979.
[20]H. Heegn, "Model Describing the Resistance Against Structural Changes and the Hardness of Crystalline Solids," *Crystl. Res. Technol.*, **22**, 1193–203 (1987).
[21]D. Tromans and J. A. Meech, "Fracture Toughness and Surface Energies of Minerals: Theoretical Estimates for Oxides, Sulphides, Silicates and Halides," *Miner. Eng.*, **15**, 1027–41 (2002).
[22]Z. Ding, S. Zhou, and Y. Zhou, "Hardness and Fracture Toughness of Brittle Materials: A Density Functional Theory Study," *Phys. Rev. B*, **70**, 184117, 4pp (2004).
[23]W. W. Gerberich, W. H. Mook, C. B. Carter, and R. Ballarini, "A Crack Extension Force Correlation for Hard Materials," *Int. J. Fracture*, **148**, 109–14 (2007).
[24]S. J. Lloyd, et al., "Observations of Nanoindents via Cross-Sectional Transmission Electron Microscopy: A Survey of Deformation Mechanisms," *Proc. Roy. Soc. A*, **461**, 2521–43 (2005).
[25]I. Yonenga, "Hardness, Yield Strength and Dislocation Velocity in Elemental and Compound Semiconductors," *Mater. Trans.*, **46**, 1979–85 (2005).
[26]K. Mizushima, M. Tang, and S. Yip, "Toward Multiscale Modeling: The Role of Atomistic Simulations in the Analysis of Si and SiC Under Hydrostatic Compression," *J. Alloys Compounds*, **279**, 70–4 (1998).
[27]S. G. Roberts and P. B. Hirsch, "Modelling the Upper Yield Point and the Brittle-Ductile Transition of Silicon Wafers in Three-Point Bend Tests," *Philos. Mag. A*, **86**, 4099–116 (2006).
[28]B. W. Dodson and J. Y. Tsao, "Stress-Dependence of Dislocation Glide Activation Energy in Single-Crystal Silicon-Germanium Alloys up to 2.6 GPa," *Phys. Rev. B*, **38**, 12383–7 (1988).
[29]M. Brede and P. Haasen, "The Brittle-to-Ductile Transition in Doped Silicon as a Model Substance," *Acta Metall.*, **36**, 2003–8 (1988).
[30]E. A. Stach and R. Hull, "Enhancement of Dislocation Velocities by Stress-Assisted Kink Nucleation at the Native Oxide/SiGe Interface," *Appl. Phys. Lett.*, **79**, 335–7 (2001).
[31]R. Hull, J. C. Bean, L. J. Peticolas, B. E. Weir, K. Prabakaran, and T. Ogion, "Misfit Dislocation Propagation Kinetics in GeSi/Ge (100) Heterostructures," *Appl. Phys. Lett.*, **65**, 327–9 (1994).
[32]A. R. Beaber, et al., "Smaller is Tougher," *Philos. Mag.*, **91**, 1179–89 (2010).
[33]P. Pirouz, J. L. Demenet, and M. H. Hong, "On Transition Temperatures in the Plasticity and Fracture of Semiconductors," *Philos. Mag. A*, **81**, 1207–27 (2001).
[34]M. D. Drory, J. W. Ager III, T. Suski, I. Grzegory, and S. Porowski, "Hardness and Fracture Toughness of Bulk Single Crystal Gallium Nitride," *Appl. Phys. Lett.*, **69**, 4044–6 (1996).
[35]H. Idrissi, G. Regula, M. Lancin, J. Douin, and B. Pichaud, "Study of Schockley Partial Dislocation Mobility in Highly N-Doped 4H-SiC by Cantilever Bending," *Phys. Stat. Sol. (c)*, **2**, 1998–2003 (2005).
[36]J. A. Patten, W. Gao, and K. Yasuto, "Ductile Regime Nanomachining of Single Crystal Silicon Carbide," *J. ASME*, **127**, 522–32 (2005).
[37]P. Pirouz, M. Zhang, J.-L. Demenet, and H. M. Hobgood, "Transition from Brittleness to Ductility in SiC," *J. Phys. Cond. Matter*, **14**, 12929–45 (2002).
[38]Cree Catalog, MAT-CATALOG.00P. 2011, Cree Inc., Durham, NC.
[39]J. W. Lee, M. Skowronski, E. K. Sanchez, and G. Chung, "Origin of Basal Plane Bending in Hexagonal Silicon Carbide Single Crystals," *J. Cryst. Growth*, **310**, 4126–31 (2008).
[40]J. L. Demenet, et al., "Microstructures of 4H–SiC Single Crystals Deformed Under Very High Stresses," *J. Phys.: Condens. Matter*, **14**, 12961–6 (2002).
[41]K. Maeda, K. Suzuki, and M. Ishihara, "Recombination Enhanced Dislocation Glide in Silicon Carbide Observed in-Situ by Transmission Electron Microscopy," *Microsc. Microanal. Microstruct.*, **4**, 211–20 (1993).
[42]L. Riester, R. J. Bridge, and K. Breder, "Characterization of Vickers, Berkovich, Spherical and Cube Cornered Diamond Indenters by Nanoindentation and SFM," *MRS Symp. Proc.*, **522**, 45–50 (1998).
[43]A. Galeckas, J. Linnros, and P. Pirouz, "Recombination-Induced Stacking Faults: Evidence for a General Mechanism in Hexagonal SiC," *Phys. Rev. Lett.*, **96**, 025502, 4pp (2006).
[44]H. Idrissi, B. Pichaud, G. Regula, and M. Lancin, "30 Degree Si(g) Partial Dislocation Mobility in Nitrogen-Doped 4H-SiC," *J. Appl. Phys.*, **101**, 113533, 5pp (2007).
[45]R. W. Margevicius and P. Gumbsch, "Influence of Crack Propagation Direction on {110} Fracture Toughness of Gallium Arsenide," *Phil. Mag. A*, **78**, 567–81 (1998).
[46]J. Amodeo, P. Carrez, B. Devincre, and P. Cordier, "Multiscale Modeling of MgO Plasticity," *Acta Mater.*, **59**, 2291–301 (2011).
[47]A. S. Booth and S. G. Roberts, "Dislocation Activity, Stable Crack Motion and the Warm-Prestressing Effect in Magnesium Oxide," *J. Am. Ceram. Soc.*, **77**, 1457–66 (1994).
[48]C. O. Hulse and J. Pask, "Mechanical Properties of Magnesium Oxide Single Crystals in Compression," *J. Am. Ceram. Soc.*, **43**, 373–8 (1960).
[49]F. Appel, M. Bartsch, U. Messerschmidt, E. M. Nadgornyi, and S. V. Valkovskii, "Dislocation Motion and Plasticity in MgO Single Crystals," *Phys. Stat. Sol. (a)*, **83**, 179–94 (1984).
[50]S. Korte and W. J. Clegg, "Discussion of the Dependence of the Effect of Size on the Yield Stress in Hard Materials Studied by Microcompression of MgO," *Philos. Mag.*, **91**, 1150–62 (2011).
[51]G. M. Pharr, "Measurement of Mechanical Properties by Ultra-Low Load Indentation," *Mater. Sci. Eng., A*, **253**, 151–9 (1998).
[52]W. C. Oliver and G. M. Pharr, "Measurement of Hardness and Elastic Modulus by Instrumented Indentation: Advances in Understanding and Refinements to Methodology," *J. Mater. Res.*, **19**, 3–20 (2004).
[53]A. S. Booth, M. Ellis, S. G. Roberts, and P. B. Hirsch, "Dislocation-Controlled Stable Crack Growth in Mo and MgO," *Mater. Sci. Eng., A*, **164**, 270–4 (1993).
[54]S. I. Karato, Z. Wang, B. Liu, and K. Fujino, "Plastic Deformation of Garnets: Systematics and Implications of the Rheology of the Mantle Transition Zone," *Earth Planet. Sci. Lett.*, **130**, 13–30 (1995).
[55]P. H. Boldt, J. D. Embury, and G. C. Weatherly, "Room Temperature Microindentation of Single-Crystal $MoSi_2$," *Mater. Sci. Eng., A*, **155**, 251–8 (1992).
[56]R. K. Wade and J. J. Petrovic, "Fracture Modes in $MoSi_2$," *J. Am. Ceram. Soc.*, **75**, 1682–4 (1992).
[57]M. D. Drory, C. F. Gardinier, and J. S. Speck, "Fracture Toughness of Chemically Vapor-Deposited Diamond," *J. Am. Ceram. Soc.*, **74**, 3148–50 (1991).
[58]A. L. Ruoff, "On the Yield Strength of Diamond," *J. Appl. Phys.*, **50**, 3354–6 (1979).
[59]V. L. Solozhenko, S. N. Dub, and N. V. Novikov, "Mechanical Properties of Cubic BC_2N, a New Superhard Phase," *Diam. Relat. Mater.*, **10**, 2228–31 (2001).
[60]S. Mei, A. M. Suzuki, D. L. Kohlstedt, N. A. Dixon, and W. B. Durham, "Experimental Constraints on the Strength of the Lithospheric Mantle," *J. Geophys. Res.*, **115**, B082014, 4pp (2010).

[61]K. Morita, B. N. Kim, H. Yoshida, and K. Hiraga, "Densification Behavior of a Fine-Grained $MgAl_2O_4$ Spinel During Spark Plasma Sintering (SPS)," *Scripta Mater.*, **63**, 565–8 (2010).
[62]R. Terao, J. Tatami, T. Meguro, and K. Komeya, "Fracture Behavior of AlN Ceramics with Rare Earth Oxides," *J. Eur. Ceram. Soc.*, **22**, 1051–9 (2002).
[63]W. W. Gerberich, S. K. Venkataraman, J. W. Hoehn and P. G. Marsh, *Fracture Toughness of Intermetallics Using a Micro-Mechanical Probe in Structural Intermetallics*, Edited by R. Darolia, et al. pp. 569–90. TMS, Warrendale, Pennsylvania, 1993.
[64]S. Veprek and A. S. Argon, "Towards the Understanding of Mechanical Properties of Super- and Ultra-Hard Nanocomposites," *J. Vac. Sci. Technol., B*, **20**, 650–64 (2002).
[65]T. F. Page, L. Riester, and S. V. Hainsworth, "The Plasticity Response of 6H-SiC and Related Isostructural Materials to Nanoindentation: Slip vs. Densification," *Mater. Res. Soc. Symp. P*, **552**, 113–8 (1998).
[66]H. Sumiya, K. Yamaguchi, and S. Ogata, "Deformation Microstructure of High-Quality Synthetic Diamond Crystal Subjected to Knoop Indentation," *App. Phys. Lett.*, **88**, 161904, 3 pp (2006).
[67]S. M. D. Prakash and P. M. Rao, "Microhardness Investigation on Gel-Grown Barium Cadmium Oxalate Mixed Crystals," *Cryst. Res. Technol.*, **22**, 1095–9 (1987).
[68]P. Cordier, *Dislocations and Slip Systems of Mantle Minerals*, Edited by S. I. Karato and H.-R. Wenk, pp. 137–89. Mineralogical Society of America, Washington, DC, 2002.
[69]H. Kikuchi, R. Kalia, A. Nakano, P. Vashishta, P. Branicio, and F. Shimojo, "Brittle Dynamic Fracture of Crystalline Cubic Silicon Carbide (3C-SiC) via Molecular Dynamics Simulations," *J. Appl. Phys.*, **98**, 103524, 4 pp (2005).
[70]W. C. Oliver and G. M. Pharr, "An Improved Technique for Determining Hardness and Elastic Modulus Using Load and Displacement Sensing Indentation Experiments," *J. Mater. Res.*, **7**, 1564–83 (1992).
[71]W. W. Gerberich, et al., "Superhard Silicon Nanospheres," *J. Mech. Phys. Solids*, **51**, 979–92 (2003).
[72]A. J. Wagner, "An in-Situ Analytical Scanning and Transmission Electron Microscopy Investigation of Structure-Property Relationships in Electronic Materials;" Thesis, University of Minnesota, Minneapolis, MN, 2014.
[73]Y. Mishin, D. Farkas, M. J. Mehl, and D. A. Papaconstantopoulos, "Interatomic Potentials for Monoatomic Metals from Experimental Data and *Ab Initio* Calculations," *Phys. Rev. B*, **59**, 3393–407 (1999).
[74]T. Junge and J. F. Molinari, "Plastic Activity in Nanoscratch Molecular Dynamics Simulations of Pure Aluminium," *Int. J. Plasticity*, **53**, 90–106 (2014).
[75]A. Stukowski, "Visualization and Analysis of Atomistic Simulation Data with OVITO - the Open Visualization Tool," *Modelling Simul. Mater. Sci. Eng.*, **18**, 015012, 7pp (2010).
[76]A. Stukowski and K. Albe, "Extracting Dislocations and non-Dislocation Crystal Defects from Atomistic Simulation Data," *Modelling Simul. Mater. Sci. Eng.*, **18**, 085001, 13pp (2010).
[77]P. Vashishta, R. K. Kalia, A. Nakano, and J. P. Rino, "Interaction Potential for Silicon Carbide: A Molecular Dynamics Study of Elastic Constants and Vibrational Density of States for Crystalline and Amorphous Silicon Carbide," *J. Appl. Phys.*, **101**, 1035151, 12pp (2007).
[78]J. P. Rino, et al., "Short- and Intermediate-Range Structural Correlations in Amorphous Silicon Carbide (a-SiC): A Molecular Dynamics Study," *Phys. Rev. B*, **70**, 045207, 11pp (2004).
[79]M. Mishra and I. Szlufarska, "Dislocation Controlled Wear in Single Crystal Silicon Carbide," *J. Mater. Sci.*, **48**, 1593–603 (2013).
[80]W. W. Gerberich, et al., "Nanoprobing Fracture Length Scales," *Int. J. Fracture*, **138**, 75–100 (2006).
[81]W. M. Mook, et al., "Compressive Stress Effects on Nanoparticle Modulus and Fracture," *Phys. Rev. B*, **75**, 214112, 10 pp (2007).
[82]C. S. Yan, H. K. Mao, W. Li, J. Qian, Y. Zhao, and R. J. Hemley, "Ultrahard Diamond Single Crystals from Chemical Vapor Deposition," *Phys. Status Soidi (a)*, **201**, R25–7 (2004).
[83]S. Speziale, C. S. Zha, T. S. Duffy, R. J. Hemley, and H. K. Mao, "Quasi-Hydrostatic Compression of Magnesium Oxide to 52 GPa: Implication for the Pressure-Volume-Temperature Equation of State," *J. Geophys. Res.*, **106**, 515–28 (2001).
[84]G. E. Beltz, J. R. Rice, C. F. Shih, and L. Xia, "A Self-Consistent Model for Cleavage in the Presence of Plastic Flow," *Acta Mater.*, **44**, 3943–54 (1996). □

W.W. Gerberich Arriving as an Associate Professor at the University of Minnesota, Chemical Engineering and Materials Science in 1971, Professor Gerberich followed with a distinguished academic career. Prior to that in the Aerospace Industry at Ford Aeronutronic, and Berkeley, he pioneered fracture studies of TRIP steels which eventually became lower alloy, integral members of automobiles for crash resistance. At the University, some 56 PhD students have been mentored producing 500 refereed publications. This encompasses five fields of basic research including fracture mechanics of alloys to nanoindentation of thin films of metals, ceramics and semiconductors. More recently he has emphasized length scale effects in nanoparticle investigations using *in situ* probes inside electron microscopes. Numerous honors and awards include being on the Acta Metallurgica Board of Directors and Chair (1983-1989), the Board of Governors of the NSF Instituite for Mechanics and Materials and Chair (1992-1995), the Res Mechanica Chair (2002) at KU Leuven, Belgium (2002) and the G.E. Distinguished Lecture Series at RPI, (October 2006). He is Fellow of ASM, TMS and MRS and was awarded the Outstanding Paper Award for Acta Metallugica et Materialia (1994). Recently he was in residence at ETH Zurich as Visiting Professor, Fall 2013.

Roberto Ballarini is Thomas and Laura Hsu Professor and Chair of the Department of Civil and Environmental Engineering at University of Houston. He joined the University of Houston after having served for 8 yr as James Record Chair at University of Minnesota and for twenty year as Leonard Case Professor of Engineering at Case Western Reserve University. Ballarini's multidisciplinary research focuses on the development and application of theoretical and experimental techniques to characterize the response of materials to mechanical, thermal, and environmental loads. He is particularly interested in formulating analytical and computational models for characterizing fatigue and fracture of materials and structures. His research, which has been applied to problems arising in civil engineering, mechanical and aerospace engineering, materials science, electromechanical systems, biological tissues and prosthetic design, has been featured in the popular press, including the New York Times Science Times, American Scientis, Geo and Pour La Science. His current research involves theoretical, computational and experimental studies of microelectromechanical systems (MEMS) and nanoscale biological and synthetic materials, bioinspired design of composite structures and materials, seismic-resistant structural steel systems, size effects in quasibrittle materials and structures, and the collapse of the I-35W Bridge in Minneapolis.

Eric Hintsala is currently a Ph.D. candidate at the University of Minnesota, in the Chemical Engineering and Materials Science Department, under the advisement of William Gerberich and Andre Mkhoyan. He received his bachelor's degree in Materials Science and Engineering from Michigan Technological University. His research focuses on mechanical properties of materials, using *in-situ* and *ex-situ* nanoindentation techniques to understand fundamental deformation processes. Of particular interest is the brittle-to-ductile transition in crystalline systems and how they are affected by numerous variables, including size, strain rate, and environmental effects. He plans to complete his degree in 2015 and pursue a career in industrial research.

Maneesh Mishra After finishing Bachelor of Technology in Mechanical Engineering from Indian Institute of Technology Guwahati, Maneesh worked on his PhD in Materials Science from Wisconsin Madison on Nano-scale friction and wear of ceramics using molecular dynamics simulations technique. Since graduating in 2012, he has been working as R&D Process development engineer at Micron Technology,Inc. in Boise, Idaho. As a process engineer he works on design and implementation of next generation semiconductor processing techniques, In particular, his work focuses on chemical mechanical planarization process development on state-of-the-art 300 mm high volume manufacturing tools.

Jean-François Molinari is the director of the Computational Solid Mechanics Laboratory at the Ecole Polytechnique Fédérale de Lausanne (EPFL, Switzerland). He holds appointments in the institutes of Civil Engineering and of Materials Science and Engineering. He was promoted to Full Professor in 2012, and since September 2013, is the director of the Civil Engineering Institute. In 2001, he obtained a Ph.D. in Aeronautics at the California Institute of Technology (Caltech). He held professorships in several countries including the United States (Mechanical Engineering at the Johns Hopkins University) and France (Mechanical Engineering at the Ecole Normale Supérieure de Cachan). The work conducted by Prof. Molinari takes place at the frontier between traditional disciplines and covers atomistic, continuum mechanics, and multiscale numerical methods. His research activities span the domains of damage mechanics of materials and structures, nano- and microstructural mechanical properties, and tribology. Prof. Molinari is a recipient of a 2009 ERC Starting Grant award.

Izabela Szlufarska is a professor and associate chair in the Department of Materials Science & Engineering at the University of Wisconsin (UW) – Madison. Prior to joining UW in 2004, Szlufarska held a postdoctoral position at the University of Southern California. She received PhD in physics from the University of Tennessee – Knoxville in 2002 and MS degree in physics from Wroclaw University of Technology, Poland, in 1999. Szlufarska's expertise is in computational materials science with the primary focus on nanomechanics, solid/liquid interfaces and materials for nuclear energy applications. Szlufarska received a number of professional awards, including NSF CAREER award, AFOSR Young Investigator Program Award, H. I. Romnes Faculty Fellowship and she was placed on the National Academy of Engineering list of Frontiers of Engineering.